Journal of Volcanology and Geothermal Research 285 (2014) 129–135

Contents lists available at ScienceDirect

Journal of Volcanology and Geothermal Research

journal homepage: www.elsevier.com/locate/jvolgeores

Geyser preplay and eruption in a laboratory model with a bubble trap

Esther Adelstein, Aaron Tran, Carolina Muñoz Saez, Alexander Shteinberg, Michael Manga *

[a] Department of Earth and Planetary Science, University of California, Berkeley, CA 94720–4767, USA

ARTICLE INFO

Article history:
Received 9 June 2014
Accepted 4 August 2014
Available online 17 August 2014

Keywords:
Geyser
Bubble trap
Boiling
Eruption
Conduit
Preplay

ABSTRACT

We present visual observations and temperature measurements from a laboratory model of a geyser. Our model incorporates a bubble trap, a zone in which vapor can accumulate in the geyser's subsurface plumbing, in a vertical conduit connected to a basal chamber. Analogous features have been identified at several natural geysers. We observe three types of eruptions: 1) rising bubbles eject a small volume of liquid in a weak spout (small eruption); 2) boiling occurs in the conduit above the bubble trap (medium eruption); and 3) boiling occurs in the conduit and chamber (large eruption). In the last two cases, boiling in the conduit causes a rapid hydrostatic pressure drop that allows for the rise and eruption of liquid water in a vigorous spout. Boiling initiates at depth rather than propagating downward from the surface. In a single eruption cycle, multiple small eruptions precede every medium and large eruption. At least one eruption cycle that culminates in a medium eruption (i.e., a quiescent period followed by a series of small eruptions leading up to a medium eruption) precedes every eruption cycle that culminates in a large eruption. We find that the transfer of fluid with high enthalpy to the upper conduit during small and medium eruptions is necessary to heat the upper conduit and prepare the system for the full boiling required for a large eruption. The placement of the bubble trap midway up the conduit allows for more efficient heating of the upper conduit. Our model provides insight into the influence of conduit geometry on eruption style and the importance of heat transfer by smaller events in preparing the geyser system for eruption.

1. Introduction

Geysers are springs that produce episodic eruptions of liquid water and steam. Geysers are relatively rare features on Earth, requiring a particular combination of heating, fluid supply, and subsurface structure. Broadly, the geyser eruption cycle consists of a major eruption of liquid and vapor followed by a quiescent recharge period. At some geysers, a preplay stage characterized by pulses of discharge with smaller volumes of liquid and vapor precedes major eruptions (Kieffer, 1984; Karlstrom et al., 2013; O'Hara and Esawi, 2013).

The subsurface geometry of most geysers is not well constrained, but conduit and reservoir geometries are likely important in driving geyser eruptions and modulating their evolution (Kieffer, 1989; Hutchinson et al., 1997). An early model of geyser plumbing invoked a conduit with a connected "bubble trap" that allows vapor to accumulate in the system (Mackenzie, 1811). Video observations by Hutchinson et al. (1997) at Old Faithful Geyser, Yellowstone National Park, USA, show an elongated conduit with irregular sides. Video of geyser conduit interiors in Geyser Valley, Kamchatka, Russia shows contorted conduits, suggesting the presence of regions where vapor can accumulate (Belousov et al., 2013). Vandemeulebrouck et al. (2013) identified a lateral cavity connected to the conduit of Old Faithful as the location of the source of hydrothermal tremor associated with boiling and bubble cavitation.

Laboratory models have reproduced the periodic eruptions of natural geysers and can help relate eruption cycle dynamics and conduit geometry (Honda and Terada, 1906; Anderson et al., 1978; Saptadji, 1995; Lasic, 2006). Sherzer (1933) found that convection is impeded in vertical tubes with a sufficiently low diameter-to-length ratio, resulting in uneven heating of the liquid water column. This gives rise to a "critical zone" in which local temperature approaches the boiling temperature at local pressure, allowing for the initiation of boiling at depth rather than at the surface. Subsequent laboratory models have provided information on temperature, pressure, and flow rates in the geyser system (Steinberg et al., 1982b,c; Toramaru and Maeda, 2013) and demonstrated variability in eruption style (Toramaru and Maeda, 2013).

We present temperature measurements and visual observations from a laboratory model of a geyser that incorporates a bubble trap structure in the conduit. We observe three eruption types, two of which may be analogous to preplay. Temperature records suggest that discharge from preplay events warms the conduit, preparing it for eruption. The bubble trap accelerates warming of the upper conduit. Though simpler than a natural geyser, our model provides insight into the eruption cycle in a conduit with vapor accumulation zones.

2. Methods

Our model geyser is a closed glass vessel that has been evacuated of air and partially filled with water. The model is heated from below (Fig. 1). The glass vessel consists of two reservoirs connected by a

* Corresponding author. Tel.: +1 510 643 8532; fax: +1 510 643 9980.
E-mail address: manga@seismo.berkeley.edu (M. Manga).

http://dx.doi.org/10.1016/j.jvolgeores.2014.08.005
0377-0273/

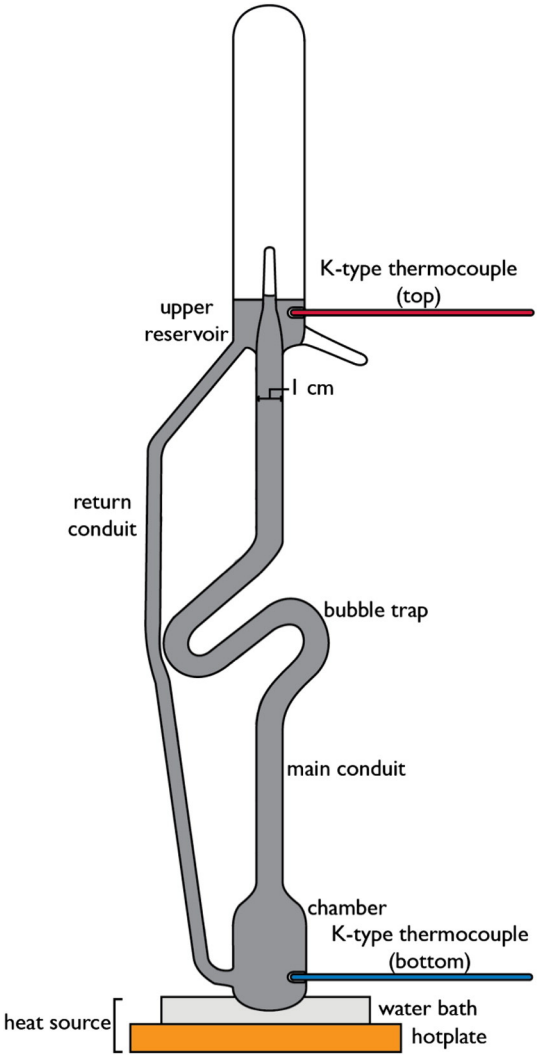

Fig. 1. Schematic of our model. Shaded regions are liquid-filled. The bubble trap divides the conduit into an upper and lower section. Thermocouples are placed in inlets in the glass. The heat source is discussed in the text.

conduit 1 cm in diameter with a central tight S-shaped bend to create a bubble trap. The conduit is thus divided into two sections: one extends into the upper reservoir and the other connects to the chamber. The total vertical separation between the top of the chamber and the top of the conduit is 24 cm. The conduit is 34 cm long.

Vapor accumulates only in the downward-facing section of the S-bend. Once bubbles exit the lower bend, they rise easily into the upper conduit; the geometry of the upward-facing section of the S-bend does not influence the eruption process. Water erupts through the upper opening of the main conduit into the upper reservoir and eventually drains back to the chamber through the return conduit. The model is not insulated from ambient conditions. A water bath serves as a heat source at the base of the model. A hotplate (Cole Parmer Vela EW-03403-10) connected to a temperature controller (Omega CN3910AKC) keeps the water bath at a constant temperature. In order to reduce evaporation, a plastic plate covers the Pyrex water bath container. A hole in the cover allows for contact between the base of the chamber and the heated water. Water level in the tray is maintained with a tube connected to a large container of room-temperature water. The temperature controller is set to an average temperature between 170 and 185 °C to keep the water bath at the boiling temperature. The only fluid in the geyser itself is that contained in the closed glass vessel. The system is therefore closed with respect to mass transfer and open with respect to heat transfer. We invert the model once while it warms in order to generate a bubble in the conduit and accelerate onset of the eruption process. Once the water bath has reached the boiling temperature and the rate of increase in bottom temperature has decreased, the model is left to run for up to 8 hours. The large container of room-temperature reservoir is refilled as needed during the course of the experiment.

K-type thermocouples are placed in cavities in the glass to record temperature at the upper reservoir ("top") and chamber ("bottom"). There is no direct contact between the thermocouples and the water in the sealed model. All measurements reflect the temperature within the glass cavities, not the temperature of the water itself. In order to verify that ambient and heat source temperatures are stable, we also record temperature at the hotplate–water–tray interface, in the heat source water tray, and in the air approximately 2 cm away from the side of the upper reservoir. Thermocouples are connected to a National Instruments (NI) TBX-68T board, which is in turn connected to a personal computer with a NI 4351 PCI card installed. The digitized temperature data is recorded with NI LabVIEW, using a modified version of the "NI 435x Continuous Buffered Acq.vi" virtual instrument. Temperature sampling interval for the five-thermocouple setup is 0.8 s. We simultaneously record video of the model using a webcam (Logitech c615 HD) connected to a personal computer to distinguish stages in the eruption process with similar temperature signatures. We also record high-speed video (60 to 160 frames per second) of individual events using a Redlake MotionPro camera and Redlake MiDAS software (version 2.1.1 R).

3. Observations of the eruption process

We identify four stages in the eruption cycle. In the following descriptions, "bubble" refers to a discrete parcel of water vapor, "Taylor bubble" to a longer bubble that occupies the entire conduit diameter except for a thin liquid film on the conduit walls, "vapor" to the vapor phase of water not visible as discrete bubbles, and "fluid" to the two-phase mixture of liquid water and water vapor.

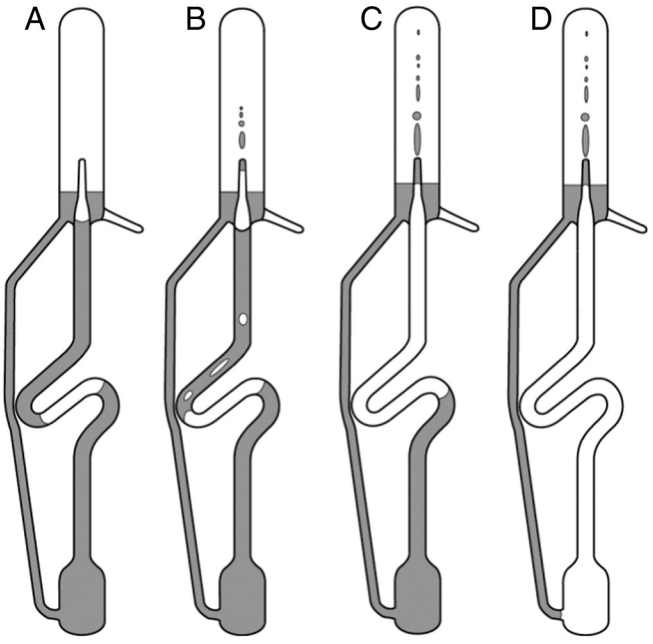

Fig. 2. Schematic of stages in the eruption cycle. Shaded regions are liquid-filled. Boiling occurs in the unshaded regions in the conduit. A. The quiescent recharge stage. B. Small eruption. C. Medium eruption. D. Large eruption. In C and D, the boiling region is a first-order approximation; Taylor bubbles rise through the conduit in a vapor-rich two-phase flow during these events. Additionally, liquid is delivered to the chamber during large eruptions (see Fig. 4).

The eruption cycle begins with the vapor accumulation stage. When a bubble nucleates in and rises from the chamber, it is trapped in the lower bend of the conduit (the bubble trap). Bubbles continue to rise from the chamber, accumulate, and coalesce into a bubble in the lower bend. As vapor accumulates, the bubble elongates and grows to occupy the entire conduit diameter in the bend (Fig. 2A). The surface remains quiescent. The vapor accumulation stage lasts for 3 to 5 minutes at the designated hotplate temperature and is identified in the bottom temperature time series as the interval of relatively smooth temperature increase following a large-amplitude temperature drop (Fig. 3).

As the chamber warms, the trapped bubble oscillates and releases bubbles upward through the conduit. Vapor occasionally reaches the top of the conduit and expels a small amount of liquid in a weak spout. We refer to this process as a "small eruption" (Fig. 2B, Supplementary Video S1). Small eruptions correspond to small-amplitude drops in bottom temperature during a general trend of temperature increase. Small eruptions separated by brief (less than one minute) periods of quiescence (the "bubbling stage") continue until a larger amount of water is erupted. Condensation forms on the walls of the upper reservoir in this stage and persists for the duration of the eruption cycle, indicating that some vapor reaches the top of the conduit.

We observe two modes of expulsion of larger volumes of water in a vigorous spout characterized by a sharp, ~5–10 °C drop in bottom temperature and a simultaneous increase in top temperature. These events last, on average, for 30 seconds, starting at the final peak in bottom temperature before the decrease and ending when the temperature drops to a minimum and starts to rise again (Fig. 3). High-speed video of these events shows a rise in liquid level in the upper reservoir, indicating that the rate of liquid drainage from the upper reservoir is lower than the rate of liquid eruption (Fig. 4). The rate of liquid drainage from the upper reservoir through the return conduit, rather than the rate of liquid eruption, limits the recharge rate. The water that remains in the upper reservoir cools between eruptions (Fig. 3).

In the more common case of significant water expulsion, boiling occurs only in the conduit above the upper boundary of the trapped bubble (Fig. 2C, Supplementary Video S2). The upper surface of the trapped bubble rises, forming a Taylor bubble that first extends over the entire length of the upper conduit. The Taylor bubble breaks up in the conduit as fluid from below rises between the Taylor bubble and the conduit walls and erupts, ultimately emptying the bubble trap. We refer to these events as "medium eruptions".

A "large eruption" occurs when the entire system boils (Fig. 2D, Supplementary Video S3). The trapped bubble lengthens, extending into the upper conduit. Once it reaches the surface, the liquid in the chamber and lower conduit boils, resulting in the eruption of newly recharged liquid at the base of the chamber. All bubbles are evacuated from the conduit during eruption. During some large eruptions, recharged water fills the chamber and boils before the eruption is complete (Fig. 4). We have observed no more than one of these events per large eruption. This process does not have a distinct signature in the temperature record. After eruption, a bubble nucleates in the bottom of the chamber and rises through the conduit to the bubble trap, restarting the process.

"Small", "medium", and "large" eruption styles refer to the visible region of boiling in the conduit and not to eruption duration, spout height,

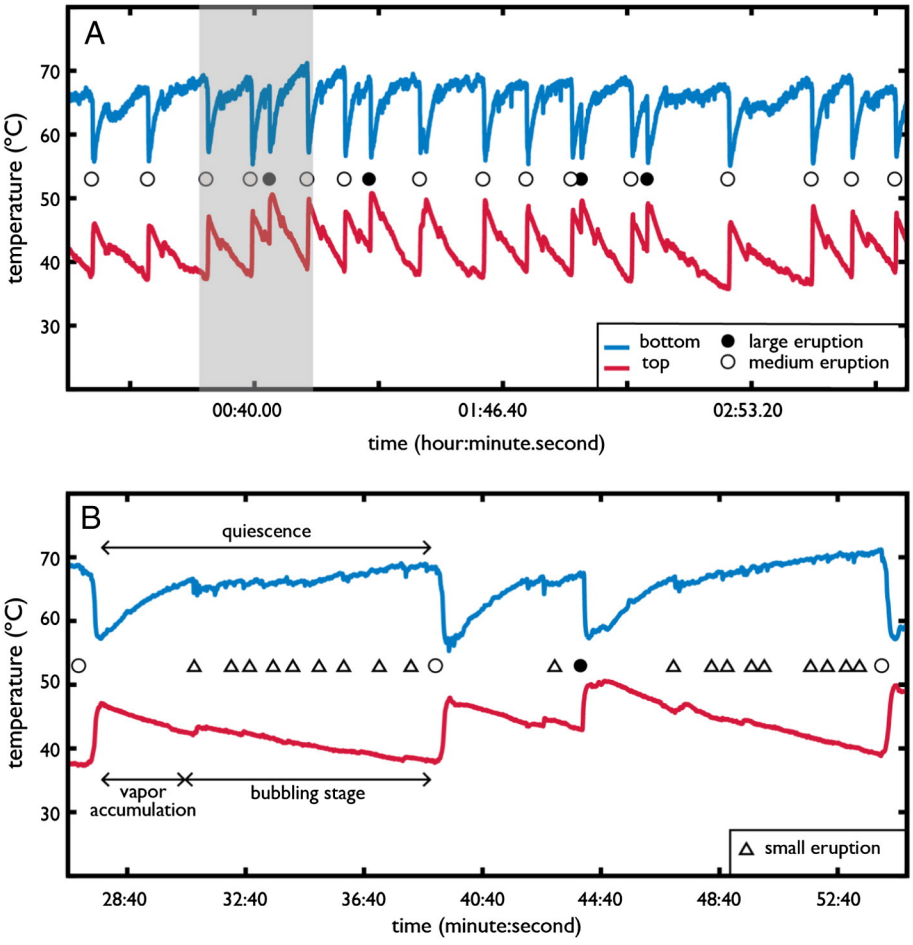

Fig. 3. A sample temperature time series with unusually short large eruption preparation stages (see Fig. 5A and B). 3B is a zoomed view of the shaded region of 3A. Bottom and top temperature measurements are plotted in blue and red, respectively. Open triangles denote small eruptions, open circles medium eruptions, and closed circles large eruptions. Vapor accumulation, small eruption, and quiescent (vapor accumulation and small eruption) stages marked with double-headed arrows. (For interpretation of the references to color in this figure legend, the reader is referred to the web version of this article.)

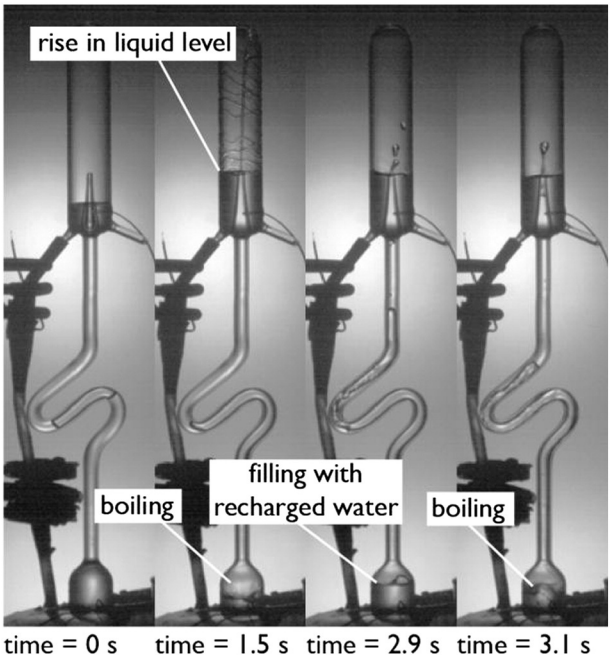

Fig. 4. Upper reservoir and recharge processes during a large eruption. During the eruption, liquid level in the upper reservoir rises, indicating a faster rate of eruption than of drainage. Recharged water enters the chamber, boils, and erupts no more than once per eruption. Images from high-speed (60 frames per second) video.

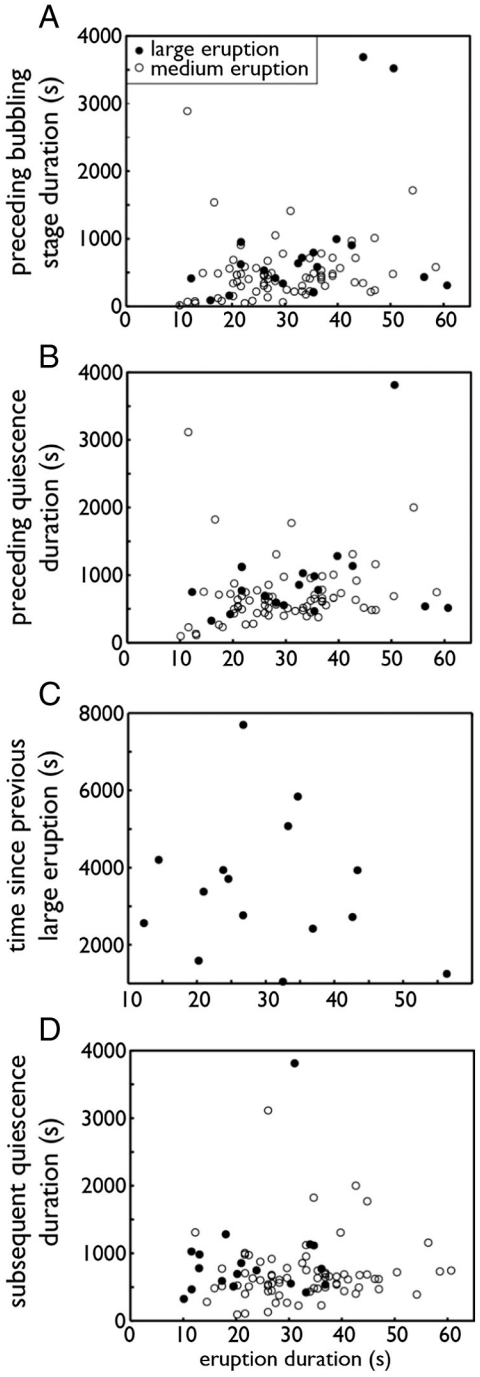

Fig. 5. Duration of preparation stages plotted against eruption duration. A shows preceding bubbling stage duration versus medium and large eruption durations, B preceding quiescence duration (recharge stage and bubbling stage) versus medium and large eruption durations, C time since previous large eruption versus large eruption duration, and D subsequent quiescence duration (recharge and bubbling stage) versus medium and large eruption durations. Open and closed circles denote medium and large eruptions, respectively. R and ρ values are summarized in Table 1.

or erupted mass. Because the height of the spout changes during an eruption and we do not measure flow rate in the conduit, we cannot assume that eruption duration is a proxy for erupted mass.

Vapor accumulation and small eruptions precede both medium and large eruptions. Consecutive large eruptions have not been observed, i.e., at least one sequence of recharge, small eruptions, and a medium eruption occurs between large eruptions (Fig. 3). We use video recordings of the entire experiment to identify small, medium and large eruptions in the temperature record. Fig. 3A and B show typical top and bottom temperature time series. The beginnings of every small, medium, and large eruption are marked. Using the annotated time series, we examine the duration of stages in the eruption cycle and the temperature at which particular events occur.

Fig. 5 shows (A) the duration of the bubbling stage compared with the duration of the subsequent medium or large eruption, (B) the duration of the quiescent stage (quiescent recharge stage and bubbling stage) compared with the duration of the subsequent medium or large eruption, (C) the time since the previous large eruption compared with the duration of the large eruption, and (D) the duration of the quiescent stage compared with the duration of the previous medium or large eruption. Because none of the data sets demonstrate a Gaussian distribution in visual inspection of histograms, both parametric (Pearson) and non-parametric (Spearman) correlation tests were conducted to test for significant correlations between preparation stage and eruption duration. The Pearson product–moment correlation coefficient (R) is a measure of the linear dependence between two variables. The Spearman's rank correlation coefficient (ρ) is defined as R between two ranked variables, and is a measure of how well the dependence between the two variables can be described by a monotonic function. ρ is less sensitive to outliers than R because the value of an outlier is limited by its rank. R and ρ values are summarized in Table 1. In all cases, neither R nor ρ is significant at the .05 level. We fail to reject the null hypothesis and find no significant correlation between the preparation stage and eruption durations.

Medium and large eruptions begin when the temperature at the bottom of the model exceeds some critical value. Critical temperature is the bottom temperature at the final peak before the sharp temperature drop of an eruption. The mean critical temperature for medium eruptions, μ_{mb}, is 69.0 °C (standard deviation $\sigma_{mb} = 1.5$ °C). The mean critical temperature for large eruptions, μ_{lb}, is 67.3 °C (standard deviation $\sigma_{lb} = 2.3$ °C) (Fig. 6). The mean top temperature at the start of medium eruptions, μ_{mt}, is 38.6 °C (standard deviation $\sigma_{mt} = 1.9$ °C). The mean top temperature at the start of large eruptions, μ_{lt}, is 40.7 °C (standard deviation $\sigma_{lt} = 3.0$ °C) (Fig. 7).

Table 1
Pearson product–moment correlation coefficient (R) and Spearman's rank correlation coefficient (ρ) values for preparation stage duration compared with eruption duration (Fig. 5).

	R	ρ
Preceding bubbling stage duration vs. large eruption duration (5A)	0.39	0.42
Preceding bubbling stage duration vs. medium eruption duration (5A)	0.02	0.21
Preceding quiescent stage duration vs. large eruption duration (5B)	0.37	0.36
Preceding quiescent stage duration vs. medium eruption duration (5B)	0.12	0.27
Time since previous large eruption vs. large eruption duration (5C)	−0.17	−0.08
Subsequent quiescent stage vs. large eruption duration (5D)	0.05	0.15
Subsequent quiescent stage vs. medium eruption duration (5D)	0.09	0.15

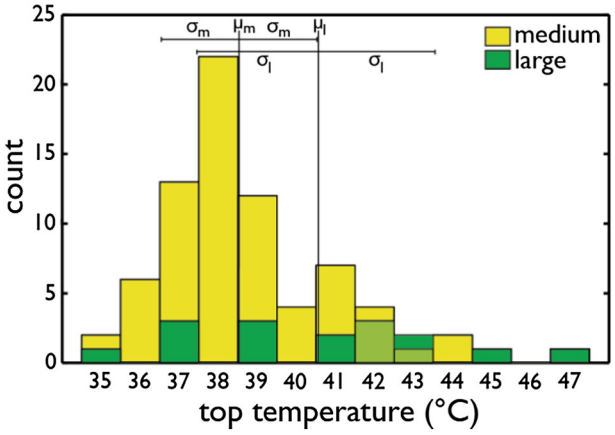

Fig. 7. Histogram of top temperature at the start of eruption and major preplay. Medium and large eruptions are plotted in yellow and green, respectively. Mean top temperature for medium eruptions (μ_{mt}) is 38.6 °C, with standard deviation (σ_{mt}) 1.9 °C. Mean top temperature for large eruptions (μ_{lt}) is 40.7 °C, with standard deviation (σ_{lt}) 3.0 °C. (For interpretation of the references to color in this figure legend, the reader is referred to the web version of this article.)

4. Discussion

We first examine the conditions under which medium and large eruptions occur. We then use these criteria to explain the roles of small eruptions, medium eruptions, and the bubble trap in transferring heat and preparing the system for eruption. Finally, we compare our observations and conclusions to those from other laboratory models and natural geysers.

Medium and large eruptions begin when enthalpy in the system is sufficiently high to allow for boiling. When liquid in the conduit boils and bubbles rise from the bubble trap, overlying water is displaced upward and ejected. The conduit becomes filled with vapor, which has relatively negligible mass. This causes a rapid hydrostatic pressure drop in the conduit below. The heated liquid below then rises up the conduit, allowing cooled water from previous eruptions to recharge the chamber. We attribute the drop in bottom temperature to the rise of warmer liquid and recharge of cooler liquid (Fig. 3). Boiling of liquid in the upper conduit can also initiate boiling in the lower conduit and chamber below. When liquid in the upper conduit boils, the liquid beneath experiences a drop in pressure. If the liquid in the lower conduit and chamber is near boiling, this pressure drop shifts the liquid to a sufficiently low pressure that the liquid boils without an increase in temperature (Kedar and Kanamori, 1998). In order to directly observe this process and rigorously interpret our results, future versions of this experiment will require measurements of pressure and temperature at multiple points within the geyser itself.

The mean top temperature at the start of large eruptions is higher than that at the start of medium eruptions. However, there is a temperature difference of at least 1 °C between each of the three modes of the distribution of top temperature at the start of large eruptions, and the central mode is within 1 °C of the mean top temperature at the start of medium eruptions (Fig. 7). We draw no conclusions regarding a typical top temperature for each eruption style. The mean critical temperature for large eruptions is lower than that for medium eruptions (Fig. 6). Intuitively, since more water boils in a large eruption than in a medium eruption, the system must be warmer in the conduit at the onset of a large eruption if the bottom temperature is cooler. Temperature measurements throughout the upper conduit of a future model are necessary to confirm this. Medium and large eruptions end when the chamber has been recharged with relatively cold erupted water and the temperature drops below boiling.

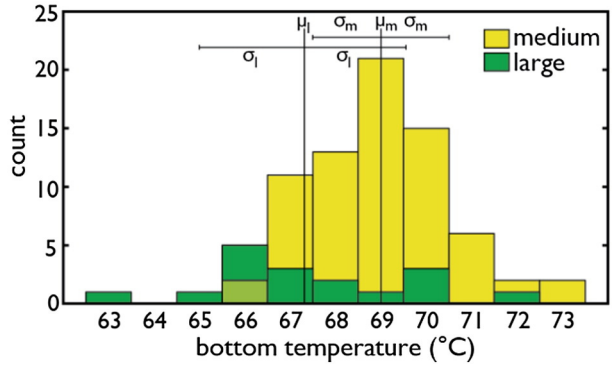

Fig. 6. Histogram of bottom temperature at the start of start of large and medium eruptions. Medium and large eruptions are plotted in yellow and green, respectively. Mean critical temperature for medium eruptions (μ_{mb}) is 69.0 °C, with standard deviation (σ_{mb}) 1.5 °C. Mean critical temperature for large eruptions (μ_{lb}) is 67.3 °C, with standard deviation (σ_{lb}) 2.3 °C. (For interpretation of the references to color in this figure legend, the reader is referred to the web version of this article.)

There is no clear significant correlation between the duration of eruption and the duration of the preceding preparation stage. Kieffer (1984) and Steinberg (1999) find that the duration of the quiescence period depends on the duration of the previous eruption, suggesting that longer eruptions more extensively deplete the system's heat and fluid supply. We do not find such a significant correlation. For a perfectly regular eruption cycle, neglecting the effect of quick recharge of cool liquid, we would expect a positive correlation between the duration of a medium or large eruption and the duration of the preceding bubbling stage. If small eruptions warm the conduit, a longer bubbling stage should allow for sustained boiling in the system. There is no significant correlation between eruption and bubbling stage durations. No significant change in R or ρ is introduced by considering the duration of the quiescent recharge stage, implying that the recharge stage is relatively unimportant in warming the conduit. Fluid flow and bubble collapse in the upper conduit do not occur during this stage. There is no significant correlation between the duration of large eruptions and time since previous large eruption. Deviations from the expected positive correlations could result from the fast recharge of the chamber with cool water from the upper reservoir. Recharge rate likely affects eruption duration. Insufficient heat supply to the chamber prevents indefinite re-eruption of recharged water. Inflow of cool water may prevent boiling at depth even if conditions in the upper conduit are such that boiling could otherwise continue elsewhere in the system.

In order to understand the importance of heat transfer from small and medium eruptions in the context of natural geysers, we compare small and medium eruptions with events at geysers called preplay. In the literature (e.g., Kieffer, 1984; Karlstrom et al., 2013), preplay is generally defined as the stage of small pulses of expulsion of fluid that

follows the quiescent recharge stage and continues until eruption. By this definition, the stage of small eruptions is the preplay stage for medium and large eruptions. However, we must also consider the differences between medium and large eruptions in our discussion of heat transfer and preparation for eruption. Because no consecutive large eruption cycles are observed, we conclude that at least one medium eruption cycle is required to prepare the conduit for a large eruption. Though medium eruptions are not strictly preplay events as defined above, i.e. they are not immediately followed by a large eruption, medium eruption cycles are pre-eruptive stages characterized by less vigorous boiling than large eruptions. In this respect, medium eruptions are preplay events for large eruptions. In the following discussion, we refer to small and medium eruptions as minor and major preplay events, respectively.

The small ratio of conduit diameter to length in the vertical sections of the conduit (lower = 1/8; upper = 1/9) likely impedes convection currents when bubbles do not rise and perturb the liquid water column, keeping the chamber and lower conduit warm relative to the upper conduit (Sherzer, 1933). The trapped bubble also limits convective heat and mass exchange between the upper and lower parts of the conduit. Preplay events disrupt the trapped bubble and transport relatively warm vapor and liquid with high enthalpy up the conduit and evacuate cold water, warming the conduit and preparing it for the boiling required for a larger eruption. Heat is transferred to the conduit walls by convection when vapor and liquid rise during preplay events and eruptions. Heat is also transferred when rising bubbles collapse in the conduit. The bubble trap allows vapor to accumulate midway up the conduit. Vapor released from this location transfers its latent heat to the upper conduit. Transfer of latent heat warms the upper conduit faster than does advection of heat by the liquid. The bubble trap allows for preplay that more efficiently warms the upper conduit, accelerating the eruption cycle.

Our model is unique among laboratory models in that it incorporates a bubble trap structure in the conduit. Previous models, all with straight conduits, have allowed vapor to accumulate only in the chamber, the upper bound of which is delineated by a constriction leading to the conduit (Anderson et al., 1978; Steinberg et al., 1982b,c; Saptadji, 1995; Lasic, 2006; Toramaru and Maeda, 2013). Additionally, our model is a closed system with respect to mass transfer and the contained fluids are subject to a confining pressure (a sealed vessel evacuated of air). In most of the models cited above, the geyser body is not sealed and contents are subject to ambient pressure conditions. Nevertheless, several aspects of the eruption process in our model match those observed in other lab models. The preparation stage of the model geyser cycle is characterized by the nucleation of bubbles at depth that subsequently rise and collapse in the conduit (Anderson et al., 1978; Saptadji, 1995). A rapid hydrostatic pressure drop from boiling in the upper conduit results in ejection of liquid and boiling at depth (Anderson et al., 1978; Steinberg et al., 1982b; Saptadji, 1995; Toramaru and Maeda, 2013). Anderson et al. (1978) observe strong low-frequency tremors from motion of the liquid water column and attribute this motion to intermittent modulation of boiling at depth. A similar process may cause the oscillation of the trapped bubble in our model. Bubbles that nucleate in the chamber displace liquid in the lower conduit. Motion of the liquid water column in the lower conduit causes motion of the trapped bubble. Upward motion of the liquid water column results in influx of relatively cool water from the recharge conduit, which delays further boiling in the chamber.

Toramaru and Maeda (2013) have also identified distinct eruption styles: jetting (vigorous liquid spout with spray) and flow (shorter spout, no spray). They find that eruption duration (in this case, a proxy for erupted mass) and frequency of occurrence of each style depends on basal water temperature in the model, with higher temperatures favoring jet eruptions and lower temperatures favoring flow eruptions. A warmer system can boil more extensively, resulting in a more vigorous eruption. We observe three eruption styles at a constant basal heat source temperature. If the extent to which the system is heated controls the type of eruption that occurs, fluid motion in previous events must introduce the variability in the heating of the system required for distinct eruption styles.

Observations of natural geysers indicate that at least some geyser conduits have contorted channels with irregular surfaces (Hutchinson et al., 1997; Belousov et al., 2013). The geometry of the bubble trap and its position relative to the conduit are also complex. The bubble trap at Old Faithful is a cavity connected to the main conduit (Vandemeulebrouck et al., 2013). Similar plumbing structures have been proposed for the Kamchatka geysers (Belousov et al., 2013). Our laboratory model is a simple approximation of the contorted conduit bubble trap configuration. The conduit walls are smooth, and vapor accumulates in the conduit itself. The large elongated bubbles that form in our model may not be stable in natural geyser conduits. Irregular conduit walls and large conduit diameters may prevent the development, oscillation, and motion of single large bubbles, while still allowing for the accumulation of vapor in the conduit.

Our experiments were motivated by trying to understand some of the processes that govern eruption style and periodicity in natural geysers. In the remainder of the discussion we compare and contrast insights from our laboratory experiments with observations and measurements at natural geysers. We emphasize that many of the inferences must remain speculative given differences in scaling and boundary conditions.

The activity within the bubble trap in our model throughout the eruption cycle shares similarities to that inferred at Old Faithful. Following an eruption at Old Faithful, tremor sources are located in the cavity, indicating vapor recharge; as the next eruption approaches, the tremor sources move toward the conduit (Vandemeulebrouck et al., 2013). We observe a similar migration of activity: the bubble trap fills before vapor is transported to the upper conduit in the bubbling stage. Vandemeulebrouck et al. (2013) observe harmonic oscillations at the depth of the tremor source, which they attribute to free oscillations of the liquid water column in the conduit above the compressible, vapor-rich fluid in the bubble trap. In our model, liquid level in the upper conduit oscillates when the trapped bubble expands and contracts in the bubble trap. Hutchinson et al. (1997) observe conduit temperature oscillations similar to the tremor source oscillations. They interpret the oscillations to be the result of local convection currents. No such pattern is clear in our temperature records; temperature oscillations coincide with small eruptions. Our model may have too narrow a conduit to develop convection currents detectable in temperature records and hence primarily reflects heat transfer by fluid eruption or bubble collapse. Bubble collapse in the conduit of Old Faithful is documented in seismic records (Kedar and Kanamori, 1998; Vandemeulebrouck et al., 2013). Bubble collapse has also been filmed in the conduit of Geyser Bol'shoy, Kamchatka (Belousov et al., 2013; supplementary videos S1–S3).

Data from Old Faithful (Hutchinson et al., 1997) show a rapid temperature increase in the conduit as hot fluid from below rises in an eruption. This agrees with temperature records from eruptions in our model. Temperature records from the conduits of Old Faithful and Geysir in Iceland (Birch and Kennedy, 1972) show the development of a critical zone at over ten meters depth. The temperature profile first intersects the assumed boiling curve at depth. Other observations of natural geysers also indicate that deep subsurface heat transfer controls the initiation of eruption. The interval between eruptions at some geysers (cone geysers, not pool geysers) does not respond to changes in wind speed or air temperature (Hurwitz et al., 2014), suggesting that subsurface processes (e.g., initiation of boiling at depth and activity in bubble trap structures) govern variability in the geyser cycle. Likewise, boiling in our model starts at depth (in the chamber or conduit), rather than propagating downward from the surface.

It has been suggested that minor eruptions prepare the system for major eruptions at some natural geysers. El Cobreloa geyser in the El

Tatio geyser field, Chile has both minor eruptions, in which bubbles collapse in the conduit and a relatively small volume of liquid is ejected at the surface, and major eruptions, in which a vigorous liquid-dominated eruption transitions to energetic steam discharge. Minor eruptions occur at regular intervals and become progressively more vigorous as a major eruption approaches (Namiki et al., 2014). Namiki et al. (2014) conclude that each minor eruption changes conditions in the conduit, preparing the system for a major eruption.

Chamber heating and recharge are the greatest limitations of our model in reproducing a natural geyser eruption cycle. Most geyser models and observations suggest inflow and subsequent mixing of hot and cold fluids (Steinberg et al., 1982a,b,c; Kieffer, 1984) or heat conduction through wall rock (Kieffer, 1984; Ingebritsen and Rojstaczer, 1993; Namiki et al., 2014) in heating the chamber and conduit, even at relatively shallow (upper conduit) depths. In our model, heating occurs at the base of the chamber only. Recharge in our model is relatively cold, occurs quickly, and begins during an eruption. Recharge in natural geysers is a complex process and depends on conditions in the geyser plumbing and the local hydraulic system (Birch and Kennedy, 1972; Ingebritsen and Rojstaczer, 1996; Hutchinson et al., 1997; Shteinberg et al., 2013). At the Yellowstone geysers and geysering wells, erupted water is not immediately recycled into the geyser system and is instead transported via outflow channels away from the geyser field (Kieffer, 1984; Hutchinson et al., 1997; Lu et al., 2005; Rudolph et al., 2012; Karlstrom et al., 2013). In natural geysers, erupted vapor does not immediately condense and reenter the system.

In our model, mass neither enters nor leaves the system. The fast recharge of the erupted volume of liquid through the secondary conduit may shorten the interval between eruptions as compared with real geysers, where fluid returns to the system much more slowly. Conversely, inflow of relatively cool water from the upper reservoir during the recharge and bubbling stages may delay the onset of boiling in the system. As previously discussed, fast recharge may also affect eruption duration.

5. Conclusions

Our model provides insight into the roles of preplay and the bubble trap structure in the geyser eruption process. The transport of vapor up the conduit in preplay events warms the conduit, moving the system closer to the boiling state required for eruption. The position of the bubble trap structure allows for vapor accumulation below the upper conduit and episodic release of the vapor and its enthalpy.

Supplementary data to this article can be found online at http://dx.doi.org/10.1016/j.jvolgeores.2014.08.005.

Acknowledgments

We thank A. Toramaru and A. Belousov for thoughtful reviews and S. Hurwitz, A. Namiki, R. Sohn, J. Vandemeulebrouck, and C.Y. Wang for feedback on an earlier version of this manuscript. This work is supported by NSF EAR 1114184.

References

Anderson, L.W., Anderegg, J.W., Lawler, J.E., 1978. Model geysers. Am. J. Sci. 278, 725–738.
Belousov, A., Belousova, M., Nechayev, A., 2013. Video observations inside conduits of erupting geysers in Kamchatka, Russia, and their geological framework: implications for the geyser mechanism. Geology 41 (7). http://dx.doi.org/10.1130/G33366.1.
Birch, F., Kennedy, G.C., 1972. Notes on geyser temperatures in Iceland and Yellowstone National Park. In: Heard, H.C., Borg, I.Y., Carter, N.L., Raleigh, C.B. (Eds.), Flow and fracture of rocks. Geophysical Monograph Series. 16. American Geophysical Union, Washington, D.C., pp. 329–336.
Honda, K., Terada, T., 1906. On the geyser in Atami, Japan. Phys. Rev. 22, 300–311.
Hurwitz, S., Sohn, R.A., Luttrell, K., Manga, M., 2014. Triggering and modulation of geyser eruptions in Yellowstone National Park by earthquakes, earth tides, and weather. J. Geophys. Res. Solid Earth 119. http://dx.doi.org/10.1002/2013JB010803.
Hutchinson, R.A., Westphal, J.A., Kieffer, S.W., 1997. In situ observations of Old Faithful Geyser. Geology 25, 875–878.
Ingebritsen, S., Rojstaczer, S., 1993. Controls on geyser periodicity. Science 262, 889–892.
Ingebritsen, S., Rojstaczer, S., 1996. Geyser periodicity and the response of geysers to deformation. J. Geophys. Res. 101, 891–905.
Karlstrom, L., Hurwitz, S., Sohn, R., Vandemeulebrouck, J., Murphy, F., Rudolph, M.L., Johnston, M.J.S., Manga, M., Blaine McCleskey, R., 2013. Eruptions at Lone Star Geyser, Yellowstone National Park, USA: 1. Energetics and eruption dynamics. J. Geophys. Res. Solid Earth 118. http://dx.doi.org/10.1002/jgrb.50251.
Kedar, S., Kanamori, H., 1998. Bubble collapse as the source of tremor at Old Faithful Geyser. J. Geophys. Res. 103 (B10), 24283–24299.
Kieffer, S.W., 1984. Seismicity at Old Faithful Geyser: an isolated source of geothermal noise and possible analogue of volcanic seismicity. J. Volcanol. Geotherm. Res. 22, 59–95.
Kieffer, S.W., 1989. Geologic nozzles. Rev. Geophys. 27 (1), 3–38.
Lasic, S., 2006. Geyser model with real-time data collection. Eur. J. Phys. 27, 995–1005. http://dx.doi.org/10.1088/0143-0807/27/4/031.
Lu, X., Watson, A., Gorin, A.V., Deans, J., 2005. Measurements in a low temperature CO_2-driven geysering well, viewed in relation to natural geysers. Geothermics 34, 389–410.
Mackenzie, G., 1811. Travels in the Island of Iceland, Edinburgh. vol. 27. Alam and Company, Edinburgh.
Namiki, A., Muñoz Saez, C., Manga, M., 2014. El Cobreloa: a geyser with two distinct eruption styles. J. Geophys. Res. 119. http://dx.doi.org/10.1002/2014JB011009.
O'Hara, K.D., Esawi, E.K., 2013. Model for the eruption of the Old Faithful Geyser, Yellowstone National Park. GSA Today 23 (6), 4–9. http://dx.doi.org/10.1130/GSATG166A.1.
Rudolph, M., Manga, M., Hurwitz, S., Johnston, M., Karlstrom, L., Wang, C.-Y., 2012. Mechanics of Old Faithful Geyser, Calistoga, California. Geophys. Res. Lett. 39, L24308. http://dx.doi.org/10.1029/2012GL054012.
Saptadji, N.M., 1995. Modeling of Geysers. (Ph.D. thesis) Auckland, New Zealand, University of Auckland, (403 pp.).
Sherzer, W.H., 1933. An interpretation of Bunsen's Geyser Theory. J. Geol. 41 (5), 501–512.
Shteinberg, A., Manga, M., Korolev, E., 2013. Measuring pressure in the source region for geysers, Geyser Valley, Kamchatka. J. Volcanol. Geotherm. Res. 264, 12–16. http://dx.doi.org/10.1016/j.volgeores.2013.07.012.
Steinberg, A.S., 1999. An experimental study of geyser eruption periodicity. Dokl. Phys. 44 (5), 47–50.
Steinberg, G.S., Merzhanov, A.G., Steinberg, A.S., Rasina, A.A., 1982a. Geyser process: its theory, modeling, and field experiment. Part 1. Theory of the geyser process. Modern Geol. 8, 67–70.
Steinberg, G.S., Merzhanov, A.G., Steinberg, A.S., Rasina, A.A., 1982b. Geyser process: its theory, modeling, and field experiment. Part 2. A laboratory model of a geyser. Modern Geol. 8, 71–74.
Steinberg, G.S., Merzhanov, A.G., Steinberg, A.S., Rasina, A.A., 1982c. Geyser process: its theory, modeling, and field experiment. Part 3. On metastability of water in geysers. Modern Geol. 8, 75–78.
Toramaru, A., Maeda, K., 2013. Mass and style of eruptions in experimental geysers. J. Volcanol. Geotherm. Res. 257, 227–339.
Vandemeulebrouck, J., Roux, P., Cros, E., 2013. The plumbing of Old Faithful Geyser revealed by hydrothermal tremor. Geophys. Res. Lett. 40, 1989–1993. http://dx.doi.org/10.1002/grl.50422.